

Characterization of a Reversible Thermoresponsive Gel and Its Application to Oligonucleotide Separation

Jun Zhang,[†] Marcus Gassmann,[‡] Xuming Chen,[†] Christian Burger,[†] Lixia Rong,[†] Qicong Ying,[†] and Benjamin Chu^{*,†}

Department of Chemistry, Stony Brook University, Stony Brook, New York 11794-3400, and Agilent Technologies, Hewlett-Packard Street 8, Waldbronn, Germany

Received March 6, 2007; Revised Manuscript Received May 14, 2007

ABSTRACT: Pluronic mixtures of F87 ($E_{61}P_{40}E_{61}$) and F127 ($E_{99}P_{69}E_{99}$), with E and P being poly(ethylene oxide) and poly(propylene oxide), respectively, have been used as effective separation media for the separation of small charged biomacromolecules, such as oligonucleotide fragments, by microchip electrophoresis. The temperature-dependent solubility of the middle block (P_{40} or P_{69}) enables a convenient micelle formation of the triblock copolymer by self-assembly, forming ordered gel-like macrolattice structures at high polymer concentrations or high temperatures. Laser light scattering (LLS) and small-angle X-ray scattering (SAXS) were used to investigate the solution behavior, including the gel structure. Micelles of the F87/F127 mixture solution at different weight ratios almost had a constant hydrodynamic radius of about 10.6 nm, except for the pure F87 solution with a hydrodynamic radius size of about 6.3 nm. The aggregation number of the micelle increased from ~ 5 to ~ 17 with an increase in the F127 content in the solution. On the basis of the SAXS results, the macrolattice symmetry of the gel-like structure could be determined. Two kinds of ordered gel structures were observed: body-centered cubic (bcc, F87-rich region) and face-centered cubic (fcc, F127-rich region). There was a transition region between them whose structure had not yet been resolved. The cubic lattice constant decreased with increasing F87 content in the mixture. Under optimized conditions, oligonucleotide sizing markers ranging from 10 to 32 bases could be separated within 40 s with one-base resolution by microchip electrophoresis.

Introduction

Triblock copolymer poly(ethylene oxide)–poly(propylene oxide)–poly(ethylene oxide) or $E_xP_yE_x$ with E, P, and subscript denoting oxyethylene, oxypropylene, and segment length, respectively, is an amphiphilic copolymer and has unique viscosity-adjustable and dynamic coating properties.^{1–3} Commercially available products of these copolymers are Pluronics (BASF) and Poxamers (ICI). At low temperatures, the triblock copolymer aqueous solution acts as a free-flowing liquid with low viscosity because the copolymer is in an unaggregated unimer state, since E and P blocks are both soluble in water, while at elevated temperatures, the solution viscosity is increased mainly due to the overlapping of the coronae of self-assembled core–shell micelles that are formed by the breakdown of hydrogen bonds between the P block and water.^{4,5} At appropriate concentration and temperature, the formed micelles can be densely packed, yielding the macrolattice of an ordered structure (gel-like state).^{6–10} Many studies on the applications of these nonionic surfactants in several fields, such as detergency,^{11–13} emulsification,^{14–16} DNA separation,^{3,10,17–21} and drug delivery,^{22–29} have been reported.

The design and synthesis of oligonucleotides have increased dramatically in recent years because oligonucleotide synthesis and antisense technology have opened another door for modern drug development.^{30,31} Isis' Vitravene is the first oligonucleotide drug on the market for the treatment of retinitis in AIDS patients.³² The rapid development of potential antisense therapeutics thus presents a challenge to the analytical methodology, i.e., to develop corresponding efficient separation methods.

However, oligonucleotide fragments cannot be successfully separated according to their sizes by conventional capillary zone electrophoresis (CZE) since they have similar mobilities, independent of their chain length. In the past decades, the most commonly used methods for the quality control of synthesized oligonucleotides have been polyacrylamide (or agarose)-based slab/capillary gel electrophoresis^{33–38} and high-performance liquid chromatography (HPLC).^{39–41} The main disadvantages of these methods are time-consuming and insufficient efficiency. With completion of the Human Genome Project, the microchip electrophoresis technique appears to be promising and is almost 2 orders of magnitude faster than the conventional capillary electrophoresis.⁴² Although this platform is very efficient and has many applications in DNA analysis, the separation of oligonucleotides has remained to be a challenging problem.

Recently, we have successfully developed a reversible thermoresponsive gel system as the separation medium for oligonucleotide separation by microchip-based capillary electrophoresis.³ The system used a blend of thermoresponsive Pluronic copolymers F127 ($E_{99}P_{69}E_{99}$) and F87 ($E_{61}P_{40}E_{61}$), at certain weight fractions, to create a highly efficient oligonucleotide sieving matrix with a thermally tunable solution viscosity. Both Pluronic F127 ($E_{99}P_{69}E_{99}$) and F87 ($E_{61}P_{40}E_{61}$) consist of 70% poly(ethylene oxide) and 30% poly(propylene oxide). Although F127 was studied by many research groups and found many applications, F87 attracted little attention and was first employed as a sieving matrix for oligonucleotide separation by our research group.^{43,44} Single-stranded oligonucleotide sizing markers ranging from 8 to 32 base could be separated in a 1.5 cm long separation channel by the mixture solution in its gel-like state.³

The sieving ability of the Pluronic mixture solution appears to be related to the macrolattice ordered structure formed by the polymer gel matrix. In this work, static light scattering (SLS), dynamic light scattering (DLS), and small-angle X-ray scattering

* Corresponding author: Tel +631-632-7928; Fax +631-632-6518; e-mail bchu@notes.cc.sunysb.edu.

[†] Stony Brook University.

[‡] Agilent Technologies.

(SAXS) were used to characterize both the solution and gel properties. Through these experiments, the type of ordered structure in the gel-like state, the lattice constant, and the size of the micelle have been revealed. With this data, it is possible to partially quantify the sieving ability of the Pluronic mixture solution and to understand the sieving mechanism of oligonucleotide separation.

Experimental Section

Materials. Pluronic F127 ($E_{99}P_{69}E_{99}$) and F87 ($E_{61}P_{40}E_{61}$) were gifts from the BASF Corp. (Parsippany, NJ). Polymer solutions were prepared by mixing preweighed triblock copolymers with $1\times$ TBE buffer (89 mM tris(hydroxymethyl)aminomethane, 89 mM boric acid, and 2 mM EDTA in Milli-Q water) to the desired concentrations (all buffer reagents were bought from Sigma-Aldrich, St. Louis, MO). The mixture was placed in the refrigerator and vortexed every few hours. Single-stranded oligonucleotide sizing markers (a set of 13 synthetic oligonucleotides ranging from 8 to 32 base with two-base increments between each oligonucleotide) were purchased from Amersham Biosciences Corp. (Piscataway, NJ). Oligonucleotides were diluted 20-fold by Milli-Q water and were heated at 95 °C for 2 min before sample injection.

Methods. Microchip Electrophoresis. Microchip electrophoresis was performed on an Agilent 2100 bioanalyzer (Agilent Technologies, Waldbronn, Germany), which used epifluorescent detection with a semiconductor laser that emitted at 635 nm. The chip was made from soda lime glass, and the effective separation length was about 1.5 cm. The experiments were carried out with our sieving matrix combined with the dye and the DNA marker, which were included in the DNA 500 reagent kit. Separation field strength was adjusted by modifying the script in the Bioanalyzer software.

Laser Light Scattering (LLS). A standard laboratory-built laser light scattering spectrometer equipped with a BI-9000 AT digital correlator and a solid-state laser (DPSS, Coherent, 200 mW, 532 nm) was used to perform LLS studies over a scattering angular range of 20°–130°. In static LLS, the angular dependence of the excess absolute time-averaged scattered intensity, using vertically polarized incident and scattered light, also known as the Rayleigh ratio $R_{vv}(\theta)$, was measured. In the limit of low concentrations (C), the weight-average molecular weight (M_w), the z -average root-mean-square radius of gyration (R_g), and the second virial coefficient (A_2) can be obtained from a Zimm plot. For dynamic light scattering (DLS), the intensity–intensity time correlation function $G^{(2)}(\tau)$ in the self-beating mode was measured. By using the CONTIN method, the normalized distribution function of the characteristic line width $G(\Gamma)$ including the mean line width $\bar{\Gamma}$ was obtained. The apparent hydrodynamic radius R_h could be obtained from the Stokes–Einstein equation. The detailed information has been described elsewhere.⁴⁵

SAXS Experiments. SAXS measurements were carried out at the X27C beamline in the National Synchrotron Light Source (NSLS), Brookhaven National Laboratory (BNL). The incident beam wavelength (λ) was tuned at 0.1371 nm. A Fuji HR-V imaging plate (200×250 mm²) was used as the detection system. The sample-to-detector distance was 1013 mm.

Viscosity Measurements. Viscosity was measured with a CC27/Q1 coaxial cylinder measuring system in an Anton Paar Physica MCR 301 rheometer. Shear rates ranged from 0.1 to 100 s⁻¹. Zero-shear rate viscosity was extrapolated from the data points.

Results and Discussion

LLS Study on F87 Properties in Dilute Solution. Amphiphilic Pluronic nonionic surfactants are a series of ethylene oxide/propylene oxide triblock copolymers with a general formula $E_xP_yE_x$. In a recent study, we found that the use of a 30% (w/v) concentration of Pluronic F127 solution in combination with the OliGreen dye could achieve the best sieving performance and the fastest separation speed for oligonucleotide separation in a very short separation channel (~ 3 cm).¹⁷ Thus,

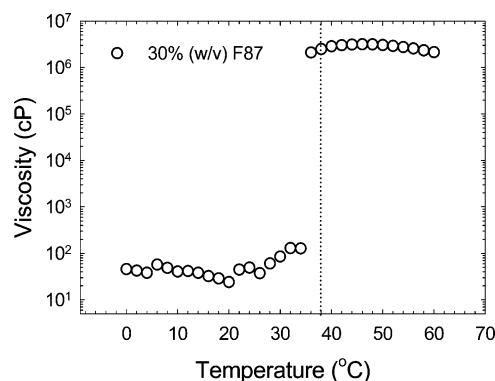


Figure 1. Temperature dependence of viscosity of 30% (w/v) F87 solution in $1\times$ TBE buffer.

a fixed concentration of 30% (w/v) was chosen for which the solution, and gel-like states were investigated in this work. Like F127 ($E_{99}P_{69}E_{99}$), F87 ($E_{61}P_{40}E_{61}$) is another Pluronic triblock copolymer. It has the same PEO/PPO ratio, namely 70% PEO and 30% PPO. It represented the first time we introduced Pluronic F87 as a component of the oligonucleotide separation matrix.³ Because of the smaller hydrophobic part in F87 when compared with F127, F87 aqueous solution has a higher phase transition temperature than that of F127 at the same concentrations. For example, a 30% (w/v) F87 solution has a gel-forming temperature of about 38 °C, while the transition temperature of 30% (w/v) F127 is about 18 °C. Figure 1 shows the temperature dependence of the zero-shear rate viscosity of 30% (w/v) F87 solution in $1\times$ TBE buffer. With increasing temperature from 0 °C, the solution viscosity decreased slightly at low temperatures due to the shrinkage of coil size caused by the increase in PPO hydrophobicity. Further increasing the temperature would cause the viscosity to increase and turn the system into a gel-like state. It should be noted that a 30% (w/v) F87 solution in $1\times$ TBE buffer had a really low viscosity of less than 50 cP at low temperatures (0–20 °C), which could enable the rapid loading of microchips under low applied pressure and hence facilitate an easier automation of the system.

In dilute solution, the micelle formation induced by either the temperature change or the concentration incremental change could be measured by an abrupt increase in the scattered intensity using static light scattering. The critical micelle temperature (cmt) is defined as the temperature at which the light scattering intensity departs significantly from the baseline intensity contributed only by unimers. Figure 2a shows typical static light scattering results for the determination of cmt at various concentrations. The y-axis is the relative excess scattered intensity I_{ex} , which is obtained from $(I - I_0)/I_{ben}$, where I , I_0 , and I_{ben} are the scattered intensity of polymer solution, solvent, and benzene, respectively. Generally the scattered intensity is measured at a scattering angle of 90°. The cmt value was estimated by the intersection of the two linear regression lines. For example, the cmt value of a F87/ $1\times$ TBE solution at the concentration of 8×10^{-3} g/mL was about 31.7 °C. Figure 2a also shows the concentration dependence of critical micelle temperature. As expected, the polymer solution at higher polymer solution concentrations had lower critical micelle temperatures. The dependence of critical micelle temperature on polymer solution concentration is plotted in Figure 2b. Because of the smaller hydrophobic section of F87, the critical micelle concentration (cmc), which could be extrapolated from Figure 2b, was relatively high at 25 °C compared to F127, which has a cmc value of 6.1 mg/mL at 25 °C.¹⁰

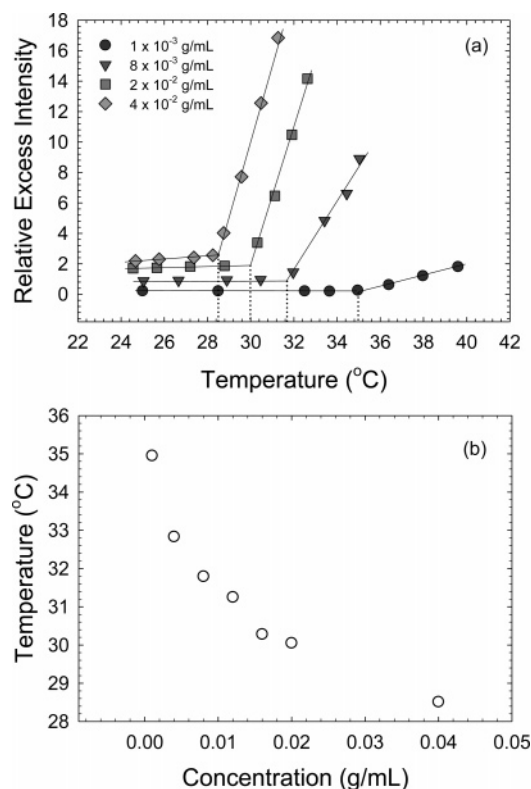


Figure 2. (a) Typical static light scattering results for the determination of critical micelle temperature (cmt) at various concentrations. (b) Dependence of cmt on polymer solution concentration.

Dynamic light scattering (DLS) measures the intensity–intensity time correlation function $G^{(2)}(\tau)$ as a function of the delay time τ . The normalized characteristic line width distribution function $G(\Gamma)$, which is related to the translational diffusion coefficient D , is obtained by the CONTIN analysis.⁴⁶ The apparent hydrodynamic radius R_h is determined from the Stokes–Einstein relation. At high temperatures, F87 forms micelles in aqueous solution due to the breakdown of hydrogen bonds between the PPO blocks and water. In our study, this micelle formation process was monitored by dynamic light scattering at a scattering angle of 30° . Figure 3 shows the plots of intensity contribution function $\Gamma G(\Gamma)$ vs the apparent hydrodynamic radius of a 4×10^{-2} g/mL F87 solution in $1 \times$ TBE buffer at four different temperatures. The average apparent R_h and the variance ($\mu_2/\bar{\Gamma}^2$) of both unimers and micelles at each temperature are listed in the corresponding panel of Figure 3. The variance is a measure for the polydispersity of the system. The distribution could be estimated by the equation $M_w/M_n \sim 1 + 4(\mu_2/\bar{\Gamma}^2)$.⁴⁷ At $\sim 25^\circ\text{C}$, a F87 solution at a concentration of 4×10^{-2} g/mL existed essentially as unimers with $R_{h,\text{app}} = 2.1$ nm. When the temperature was increased to 28.8°C , micelles were formed and coexisted with unimers whose $R_{h,\text{app}}$ value was slightly decreased to 2.0 nm. This could be expected, as increasing the temperature should increase the hydrophobicity of PPO blocks and cause a slight coil shrinkage. The unimer size distribution also became narrower with increasing temperature. The average hydrodynamic radius of micelles was estimated at 9.6 nm with a broad size distribution. The corresponding area of each peak represents the intensity contribution of each component. The weight fraction of each component in the system could be obtained from the peak area ratio assuming the total integrated area to be unity. When the temperature was increased to 29.6°C , the dynamic equilibrium between unimers and micelles was shifted in favor of micelles. Both the unimer size (1.8 nm) and micelle size (8.8 nm) were

decreased further, and the size distribution became narrower. By further increasing the temperature to 31.3°C , micelles became the dominant component. It should be noted that the micellar size and the size distribution became smaller and narrower, respectively, with increasing temperature.

The concentration effect on the hydrodynamic radius of micelle was investigated. Figure 4 shows the CONTIN analysis of DLS results on F87 and F127 triblock copolymer micelles in $1 \times$ TBE at different concentrations and 36°C . The average apparent radius (measured at a scattering angle of 30°) of F87 micelle was about 6.3 nm with a narrow size distribution, and the micelle size was relatively independent of the polymer solution concentration. The results were in agreement with previous studies.^{10,48} Higher concentrations resulted in higher micellar aggregation numbers. It is reasonable to assume that the micelle size in the gel-like state is about the same as that in dilute solution at a given temperature beyond the gel transition point. Because of the larger hydrophobic core and the longer hydrophilic block, F127 micelles had a larger size when compared with F87. The average apparent radius (at $\theta = 30^\circ$) of F127 micelle was about 10.6 nm at 36°C . The concentration dependence of the micelle size was negligible, and the size distribution was relatively narrow.

F87 Properties at Gel-like State. At high concentrations and high temperatures, F87 micelles in the $1 \times$ TBE buffer were densely packed, leading to the formation of a gel-like ordered structure. Figure 5a shows the typical SAXS intensity pattern of 30% (w/v) F87 in $1 \times$ TBE buffer at 42°C . The corresponding radially averaged 1-D profile is shown in Figure 5b. Four peaks were observed with their peak positions following a simple mathematical relation of $1:\sqrt{2}:\sqrt{3}:2$, which is characteristic for a body-centered cubic (bcc) structure. From the position of the first scattering peak s_{110} , the cubic lattice constant $a = \sqrt{2}/s_{110}$ was calculated to be about 16.9 nm. The center-to-center distance of the two closest neighboring micelles was $\sqrt{3}a/2 = 14.6$ nm. From the lattice constant of the bcc structure, the micellar aggregation number N_w could be further estimated by the equation $N_w = CN_A a^3/(2M_w)$, where C , N_A , and M_w are the polymer solution concentration (g/mL), the Avogadro number, and the molecular weight of the polymer, respectively. A 30% (w/v) F87 solution in the $1 \times$ TBE buffer at 42°C had an aggregation number of about 57, which was slightly smaller than that (~ 65) of the 21.2% F127 solution in its gel-like state.¹⁰ We tested its sieving ability and, unfortunately, it was not able to separate the oligonucleotide fragments in a 1.5 cm long separation channel that simulated the microchip condition in the Agilent Bioanalyzer 2100.³

F87 and F127 Solution Mixtures. The advantages of using a mixture of two block copolymers instead of a single copolymer are that the DNA separation resolution is highly sensitive to the copolymer block lengths. In addition, the sol–gel phase transition temperature can be tuned by changing the weight fractions of the two constituent copolymers. It is not practical to synthesize an optimal block copolymer to meet the above specifications. Our group successfully applied the triblock copolymer mixture as the sieving matrix for dsDNA separation by capillary electrophoresis.⁴⁹ A series of mixed solutions were prepared using different F87/F127 weight ratios at a fixed concentration of 30% (w/v). The chosen concentration was found to be optimal for oligonucleotide separation by capillary electrophoresis in our previous study.¹⁷

In microchip electrophoresis, the polymer solution viscosity and the gel transition temperature are important parameters. A polymer solution with low viscosity will allow the rapid loading

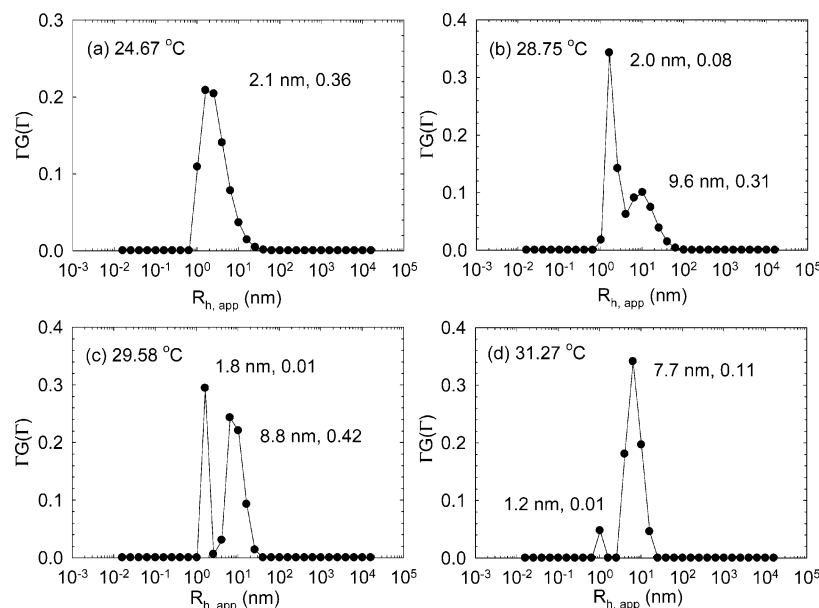


Figure 3. Plots of intensity contribution function $\Gamma G(r)$ vs apparent hydrodynamic radius of a 4×10^{-2} g/mL F87 solution in 1×TBE buffer at four different temperatures.

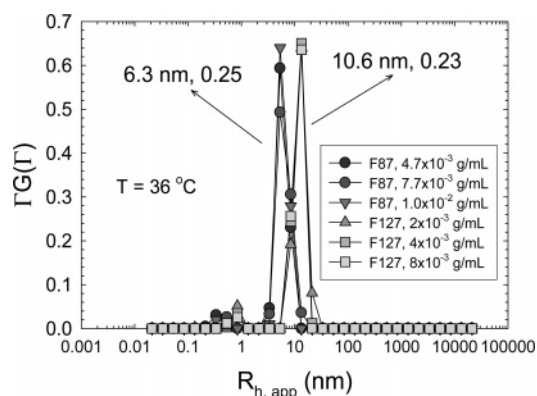


Figure 4. CONTIN analysis of DLS results on F87 and F127 triblock copolymer micelles in 1×TBE at different concentrations and 36 °C.

of polymer matrix into chip microchannels under low applied pressure and, hence, make a full automation of the system easier. An appropriate gel transition temperature will also facilitate the solution filling process and help prevent the dye and oligonucleotides from being destabilized at high temperatures. Figure 6 shows the temperature dependence of the apparent viscosity of the 30% (w/v) F87/F127 mixture solution at different weight ratios in 1×TBE buffer. The apparent viscosity was measured at a constant shear rate of 0.5 s^{-1} . Compared with the zero shear rate viscosity of 30% F87 in Figure 1, the temperature dependence of the viscosity of the mixed F87/F127 solution was similar. The solution viscosity decreased slightly in the beginning as the temperature was increased, and then increased sharply to a high value, which indicated the gel formation at a specific temperature determined by the polymer weight ratios. As shown in Figure 6, the viscosity of different F87/F127 mixture solutions was less than 100 cP at low temperatures, for example, ~ 10 °C. It was almost 2 orders of magnitude smaller than those of the conventional polyacrylamide and poly-(*N,N*-dimethylacrylamide) solution matrices used for DNA separations.⁵⁰ The sol–gel phase data of the mixture solution could also be determined from the viscosity data in Figure 6. It was observed that the LCST of the mixture solution increased with increasing F87 content at the constant concentration of 30% (w/v). The sol–gel transition temperature could be tuned

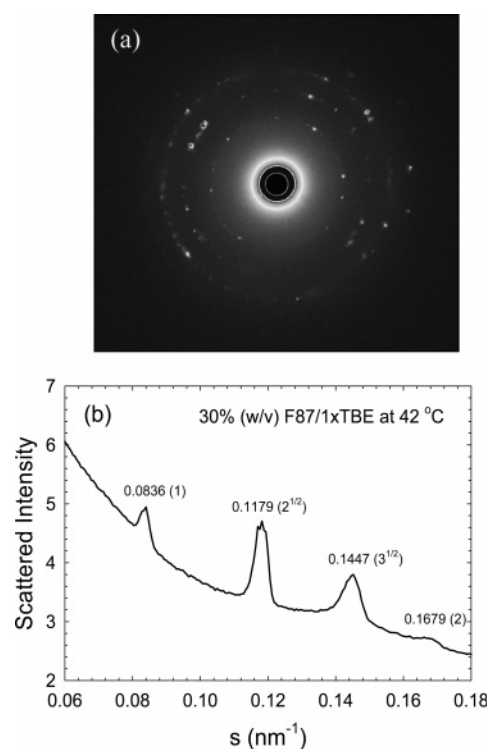


Figure 5. (a) Typical SAXS intensity pattern of 30% (w/v) F87 in 1×TBE buffer at 42 °C. (b) Corresponding radially averaged 1-D intensity profile.

over a wide range (from ~ 18 to ~ 38 °C), and the process is thermoreversible. The low viscosity and the easy-to-tune gel transition temperature are the desirable properties in microchip electrophoresis.

With increasing temperature at high polymer concentrations, the increasing hydrophobicity of the PPO block causes an increase in the total number of micelles. The resulting repulsion of the partially overlapping PEO coronae leads to a transformation to an ordered gel-like state. The ordered structures of the F87/F127 mixed solution at different weight ratios in their gel-like states were investigated by small-angle X-ray scattering (SAXS). Figure 7 shows typical SAXS intensity patterns of 30%

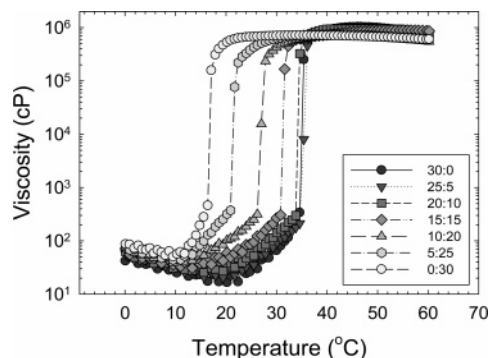


Figure 6. Temperature dependence of apparent viscosity of 30% (w/v) F87/F127 mixture solution at different weight ratios in 1×TBE buffer.

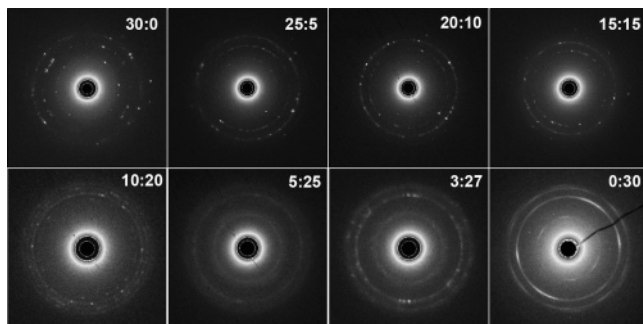


Figure 7. Typical SAXS intensity patterns of 30% (w/v) F87/F127 solution in 1×TBE at different weight ratios in their gel-like states. Three kinds of ordered structures were observed when the F127 content (weight percent) in the mixed solution was changed from 0 to 30%.

(w/v) F87/F127 solution in 1×TBE at different weight ratios in their gel-like states. Three kinds of structures were observed when the F127 content (weight percent) in the mixed solution was changed from 0 to 30%. On the basis of the peak position ratios from SAXS (radially averaged 1-D profiles from 2-D patterns), the symmetry of the gel structure could be determined. At lower F127 content (less than 50%), the mixed solution showed a body-centered cubic (bcc) structure whose peak positions followed the ratio of $1:\sqrt{2}:\sqrt{3}:2$. When the F127 content reached 66.7%, a transition state was observed. The detailed structure could not be determined at this time. By further increasing the F127 content in the mixed solution, the face-centered cubic (fcc) structure, whose peak positions followed the ratio of $1:\sqrt{4/3}:\sqrt{8/3}:\sqrt{11/3}:2$, instead of the bcc structure, was observed. With the introduction of F87 in F127, we could not only tune the gel transition temperature but also change the lattice constant of the ordered structure. Figure 8 shows the change of the lattice constant with the F87 content in the mixed solution. The lattice constant could be tuned from 17 to 28 nm by changing the F87/F127 weight ratio in the solution at a fixed concentration of 30% (w/v). It should be noted that the lattice constant at 10% F87 was estimated by assuming that the gel was in a transition state between fcc and bcc.

The solution property of F87/F127 mixed solution at dilute concentration was investigated by dynamic light scattering. Figure 9 shows an example of plots of intensity contribution function $\Gamma G(\Gamma)$ vs the apparent hydrodynamic radius, at 8×10^{-3} g/mL F87/F127 solution and a weight ratio of 1:2 in 1×TBE buffer at different temperatures. The intensity–intensity time correlation function was measured at a scattering angle of 30° . The average apparent hydrodynamic radius $R_{h,app}$ and the variance ($\mu_2/\bar{\Gamma}^2$) of both unimers and micelles at each temperature are shown in Figure 9. The temperature effect on micelle

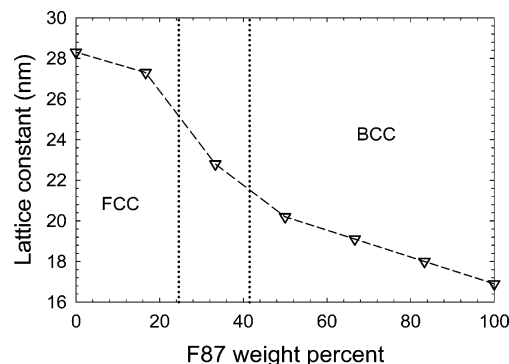


Figure 8. Change of lattice constant with F87 content in mixture solution.

size and size distribution had the same tendency as that in dilute F87 solution. At 25°C , unimers and micelles with a broad distribution coexisted in the solution. The hydrophobic interactions between PPO blocks were not strong enough so that some aggregates were very large, with sizes of more than 100 nm. As the temperature was increased, the increased hydrophobic interactions caused the unimers to shrink. Because of the minimization of free energy, the size distribution became narrower. Enhanced PPO hydrophobic interactions due to the temperature increase also shifted the equilibrium between unimers and micelles to the direction in favor of micelles, as indicated by a reduction in the integrated area of the unimer peak in Figure 9. Table 1 lists all the parameters obtained from both static and dynamic light scattering experiments. The micelles of the F87/F127 mixture solution at different weight ratios almost had a constant hydrodynamic radius of about 10.6 nm, except for the pure F87 solution with a size of about 6.3 nm. Here, the apparent hydrodynamic radius referred to the line width measurements obtained at $\theta = 30^\circ$, instead of the real hydrodynamic radius obtained by extrapolation to zero scattering angle and infinite dilution, because the micelle size was obtained at a finite concentration (Figure 4) and angular dependence (data not shown). To calculate the micellar aggregation number, we used the modified Rayleigh–Gans–Debye equation by measuring the excess Rayleigh ratio of micelles at 90° .⁵¹ The aggregation number of the micelle apparently increased from ~ 5 to ~ 17 with an increase of F127 content in the solution. It is interesting that the micellar aggregation number changed with the F127 content in the mixture solution while the micellar size was kept almost constant, as the effective hydrodynamic size was determined essentially by the longer hydrophilic block of the two block copolymers.

Microchip Electrophoresis Performance on Oligonucleotide Separation. The sieving ability of the F87/F127 mixture solution for single-stranded oligonucleotide separation was examined on the Agilent Bioanalyzer 2100, and the results were compared with those for the Agilent gel. Several kinds of kits for different size ranges have been provided by Agilent Technologies. The DNA 500 Assay Kit was the one suitable for DNA fragment sizing and quantitation ranging from 25 to 500 bp. It provided a higher resolution of smaller fragments (~ 5 bp in 25–100 bp) in comparison to other Agilent DNA sizing kits. A 30% (w/v) F87/F127 mixture solution with a weight ratio of 1:2 was used as the separation medium, which was found to be an optimized recipe for oligonucleotide separation in our previous studies. Figure 10 shows the electropherograms of oligonucleotide separation by the Agilent DNA 500 Kit (a) and our gel (b). Although the gel matrix in the DNA 500 Kit had the best resolution for smaller DNA fragments, it had no resolving power for oligonucleotides with

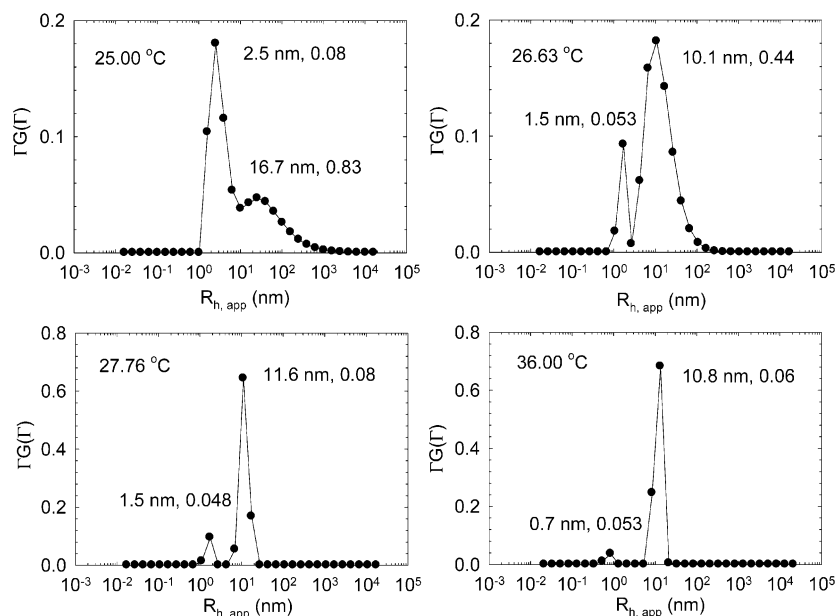


Figure 9. Plots of intensity contribution function $\Gamma G(\Gamma)$ vs apparent hydrodynamic radius of a 8×10^{-3} g/mL F87/F127 solution at a weight ratio of 1:2 in 1×TBE buffer at different temperatures.

Table 1. Laser Light Scattering Results for F87/F127 Dilute Solutions at 36 °C

F87/F127 weight ratio	30:0	25:5	20:10	15:15	10:20	5:25	0:30
micelle $R_{h,app}$ (nm)	6.3	10.4	10.5	10.5	10.8	10.7	10.6
variance (μ^2/Γ^2)	0.063	0.063	0.063	0.053	0.058	0.058	0.053
calculated M_w (10^3 g/mol)	7.7	8.5	9.3	10.1	11	12	12.6
aggregation N_w	5	6	10	13	14	17	17

a size range from 8 to 32 base at any tested electrical fields. Figure 10b illustrates the microchip electrophoresis of oligonucleotide sizing markers with our optimized gel at 37 °C under an applied electrical field strength of 325 V/cm. The 30% (w/v) F87/F127 mixture solution with a weight ratio of 1:2 had a gel transition point of about 26 °C. At 37 °C, the mixture solution was in the gel-like state, and all oligonucleotide fragments were baseline separated. One base resolution has been achieved for oligonucleotide separation by our gel in the Agilent Bioanalyzer 2100 system. To our knowledge, it is the highest resolution reported to date for oligonucleotides in the similar size range achieved by microchip electrophoresis.

For the separation of small DNA fragments, small mesh sizes are required according to the Ogston description.⁵² A polymer solution as a good separation medium requires that a polymer network above its overlap concentration would be formed with a certain effective pore size through which the DNA fragments have to migrate.⁵³ On the basis of the scaling theory,⁵⁴ the average mesh size of a concentrated polymer solution is only dependent on the polymer solution concentration given that the polymer chain length is much longer than the mesh size. We have estimated that the mesh size of the polymer solution remains almost constant when the solution concentration is beyond 10% (w/v).⁵⁰ However, the minimized mesh size due to the concentration increase may still be too large to separate very small oligonucleotide fragments. The mechanism of DNA separation by a thermoresponsive gel is different from that by conventional polymer solutions. In the gel-like state of our entangled core-shell micelles for oligonucleotide separation, there are at least four qualitatively different domains, namely the condensed PPO micellar cores, the hydrated PEO micellar shells, the entangled PEO chains in the overlapping micellar coronae among neighboring micelles, and the water-rich interstitial gaps between micelles. Highly charged oligonucleotides tend to avoid the hydrophobic micellar cores and migrate

through the hydrated poly(ethylene oxide) coronae whose chain density is not uniform and through the interstitial domains.²¹ The size of the migratable space in the gel, which is controlled by the micellar size, the micellar aggregation number, the lattice constant, and the macrolattice symmetry, may have an effect on the resolution of oligonucleotide separations. The migratable space of the 30% (w/v) F87/F127 macrolattice at a weight ratio of 1:2 happens to match closely the size range of the tested oligonucleotide fragments and, hence, showed the best performance.

Efforts have been made to extend the sieving ability of the Pluronic mixture solution for larger dsDNA fragments. The DNA sample used was a 10 bp DNA ladder ranging from 10 to 330 bp, which was obtained from Invitrogen (Carlsbad, CA). Figure 11 shows the electropherograms of the 10 bp DNA ladder by using the 30% (w/v) F87/F127 mixture at a weight ratio of 1:2 and DNA 1000 matrix provided by Agilent Co. The DNA ladder is supplied at 1 $\mu\text{g}/\mu\text{L}$ in 10 mM Tris-HCl and 1 mM EDTA buffer and diluted to 250 ng/ μL before applying it on the chip. The electropherogram in Figure 11a is a standard Bioanalyzer run using the DNA 1000 matrix as the separation medium. All fragments have been successfully separated within 80 s. However, the sieving ability of the Pluronic mixture for dsDNA was not as good. Several peaks were merged together as shown in the electropherogram in Figure 11b. This experiment showed that the extension of the sieving ability of Pluronic mixtures for dsDNA separation by microchip electrophoresis is not viable, while the 30% (w/v) F87/F127 mixture solution is an optimized sieving matrix for oligonucleotide separation by microchip electrophoresis. The upper size limit for oligonucleotide separation is found to be 60 nt at present. Figure 12 shows the separation of self-made oligonucleotide ladders

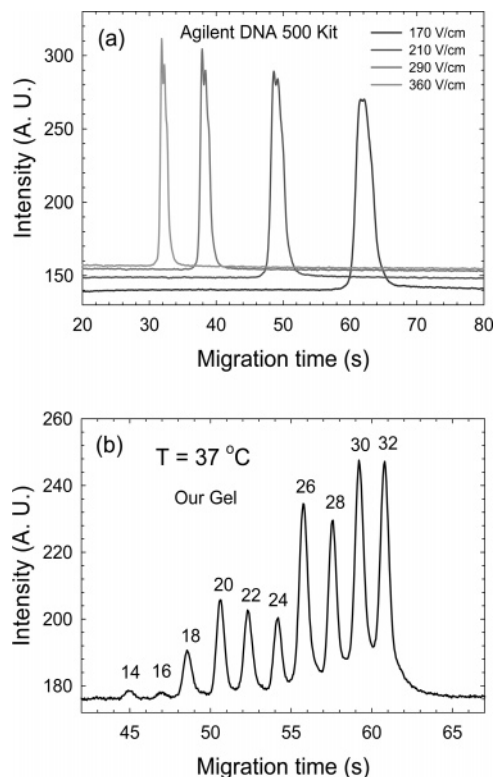


Figure 10. Electropherograms of single-stranded oligonucleotide sizing marker (10–32 base) separated by Agilent DNA 500 Kit (a) and 30% (w/v) F87/F127 mixture solution at a weight ratio of 1:2 (b) at 37 °C.

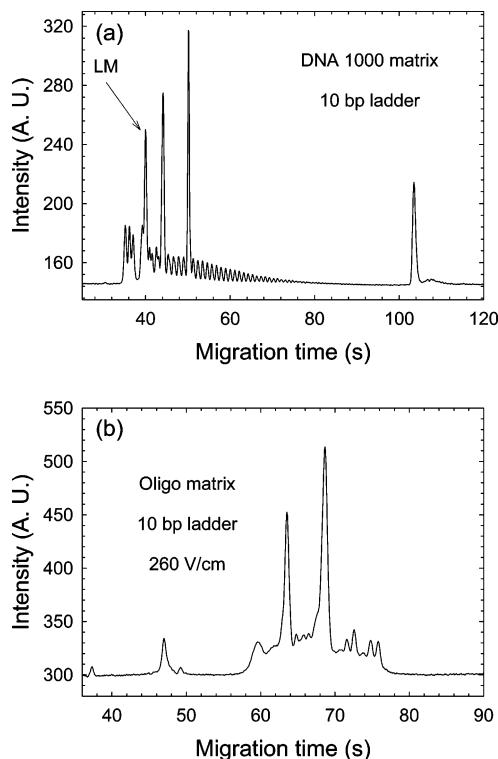


Figure 11. Electropherograms of 10 bp DNA ladder by using (a) DNA 1000 matrix provided by the Agilent Co. and (b) the 30% (w/v) F87/F127 mixture at a weight ratio of 1:2.

ranging from 35 to 60 nt with 5 base increments by the Agilent Co. The electropherogram was overlapped with that from 10–32 base fragments (Amersham ladder) and in the negative peak mode. All peaks were baseline separated. It should be noted that the dye used here is Syto-60, yielding negative peaks.

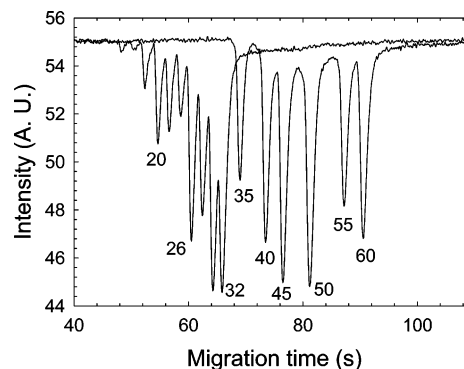


Figure 12. Overlapped electropherograms (negative peak mode) of Amersham oligonucleotide ladder (10–32 base) and Agilent self-made oligonucleotide ladder (35–60 base).

Conclusions

Pluronic F87 was first introduced as a component of the sieving matrix for oligonucleotide separation by microchip electrophoresis. The solution properties of F87 in 1×TBE buffer were investigated by laser light scattering. Because of the smaller hydrophobic part in F87 when compared with that in F127, the F87 aqueous solution has a higher critical micelle concentration and phase transition temperature than that of F127. At about 36 °C, the average apparent hydrodynamic radius ($\theta = 30^\circ$) of F87 micelles was about 6.3 nm with a narrow size distribution, and the micelle size was relatively independent of the polymer solution concentration. At high polymer concentrations and high temperatures, the F87 micelles in 1×TBE buffer were densely packed, leading to the formation of a gel-like ordered structure. A 30% (w/v) F87 solution in 1×TBE buffer at 42 °C had a body-centered cubic structure, and the aggregation number was about 57. A 30% (w/v) F87 solution in its gel-like state had no sieving ability for oligonucleotide separation. When mixed with F127, the mixture solution showed some interesting properties. The gel transition temperature could be tuned from 17 to 38 °C by varying the F87 content in the mixture. Two kinds of ordered gel structures were observed: bcc and fcc. There was a transition region between them whose structure had not yet been determined at this time. The lattice constant decreased with increasing F87 content in the mixture. The viscosity of different F87/F127 mixture solutions at low temperatures was less than 100 cP, being very convenient for the solution injection into the microchip. In dilute solution, the micelles of the mixture solution at different weight ratios had almost the same hydrodynamic radius of about 10.6 nm. The sieving ability of the mixture solution was tested in our lab-built CE system and in the Agilent Bioanalyzer. The 30% (w/v) F87/F127 mixture solution at a weight ratio of 1:2 showed the best sieving ability. Under optimized conditions, oligonucleotide sizing markers ranging from 10 to 32 base could be separated within 40 s with one base resolution.³ The extension of this sieving matrix to dsDNA separation was not viable.

Acknowledgment. B.C. gratefully acknowledges the support of this research by the National Science Foundation, Polymers Program (DMR 0454887), and by the Department of Energy (DEFG0286ER45237.23).

References and Notes

- (1) Wu, C. H.; Liu, T. B.; Chu, B. *Electrophoresis* **1998**, *19*, 231–241.
- (2) Wu, C. H.; Liu, T. B.; White, H.; Chu, B. *Langmuir* **2000**, *16*, 656–661.
- (3) Zhang, J.; Gassmann, M.; He, W. D.; Wan, F.; Chu, B. *Lab Chip* **2006**, *6*, 526–533.

- (4) Chu, B.; Wu, G. W. *Macromol. Symp.* **1995**, *90*, 251–265.
- (5) Lenaerts, V.; Triqueneaux, C.; Quarton, M.; Riegfalson, F.; Couvreur, P. *Int. J. Pharm.* **1987**, *39*, 121–127.
- (6) Mortensen, K.; Pedersen, J. S. *Macromolecules* **1993**, *26*, 805–812.
- (7) Zhang, K. W.; Khan, A. *Macromolecules* **1995**, *28*, 3807–3812.
- (8) Prud'homme, R. K.; Wu, G.; Schneider, D. K. *Langmuir* **1996**, *12*, 4651–4659.
- (9) Mortensen, K. *Macromolecules* **1997**, *30*, 503–507.
- (10) Wu, C.; Liu, T.; Chu, B.; Schneider, D. K.; Graziano, V. *Macromolecules* **1997**, *30*, 4574–4583.
- (11) Suter, H. R.; Kramer, M. G. *Soap Sanit. Chem.* **1951**, *27*, 33–6, 149.
- (12) Vaughn, T. H.; Suter, H. R.; Lundsted, L. G.; Kramer, M. G. *J. Am. Oil Chem. Soc.* **1951**, *28*, 294–9.
- (13) Pacifico, C. R.; Lundsted, L. G.; Vaughn, T. H. *Soap Sanit. Chem.* **1950**, *26*, 40–3, 73, 90.
- (14) Hong, J.-Y.; Kim, J.-K.; Song, Y.-K.; Park, J.-S.; Kim, C.-K. *J. Controlled Release* **2006**, *110*, 332–338.
- (15) Yaghmur, A.; De Campo, L.; Sagalowicz, L.; Leser, M. E.; Glatter, O. *Langmuir* **2005**, *21*, 569–577.
- (16) Zerrouki, D.; Rotenberg, B.; Abramson, S.; Baudry, J.; Goubault, C.; Leal-Calderon, F.; Pine, D. J.; Bibette, J. *Langmuir* **2006**, *22*, 57–62.
- (17) Zhang, J.; Liang, D.; He, W.; Wan, F.; Ying, Q.; Chu, B. *Electrophoresis* **2005**, *26*, 4449–4455.
- (18) Ugaz, V. M.; Lin, R.; Srivastava, N.; Burke, D. T.; Burns, M. A. *Electrophoresis* **2003**, *24*, 151–157.
- (19) Wu, C.; Liu, T.; Chu, B. *J. Non-Cryst. Solids* **1998**, *235–237*, 605–611.
- (20) Rill, R. L.; Liu, Y.; Van Winkle, D. H.; Locke, B. R. *J. Chromatogr. A* **1998**, *817*, 287–295.
- (21) Rill, R. L.; Locke, B. R.; Liu, Y.; Van, Winkle, D. H. *Proc. Natl. Acad. Sci. U.S.A.* **1998**, *95*, 1534–1539.
- (22) Frank, S. G.; Chenchow, P. C.; Sadaka, F. *Acta Pharm. Suec.* **1983**, *20*, 30–31.
- (23) Wu, H. L. S.; Miller, S. C. *Int. J. Pharm.* **1990**, *66*, 213–221.
- (24) Kabanov, A. V.; Batrakova, E. V.; Meliknubarov, N. S.; Fedoseev, N. A.; Dorodnich, T. Y.; Alakhov, V. Y.; Chekhonin, V. P.; Nazarova, I. R.; Kabanov, V. A. *J. Controlled Release* **1992**, *22*, 141–157.
- (25) Kabanov, A. V.; Nazarova, I. R.; Astafieva, I. V.; Batrakova, E. V.; Alakhov, V. Y.; Yaroslavov, A. A.; Kabanov, V. A. *Macromolecules* **1995**, *28*, 2303–2314.
- (26) Bhardwaj, R.; Blanchard, J. J. *Pharm. Sci.* **1996**, *85*, 915–919.
- (27) Barichello, J. M.; Morishita, M.; Takayama, K.; Nagai, T. *Int. J. Pharm.* **1999**, *184*, 189–198.
- (28) Morishita, M.; Barichello, J. M.; Takayama, K.; Chiba, Y.; Tokiwa, S.; Nagai, T. *Int. J. Pharm.* **2001**, *212*, 289–293.
- (29) Ricci, E. J.; Lunardi, L. O.; Nanclores, D. M. A.; Marchetti, J. M. *Int. J. Pharm.* **2005**, *288*, 235–244.
- (30) Crooke, S. T. *Annu. Rev. Med.* **2004**, *55*, 61–95.
- (31) Crooke, S. T. *Curr. Mol. Med.* **2004**, *4*, 465–487.
- (32) Orr, R. M. *Curr. Opin. Mol. Therapeutics* **2001**, *3*, 288–294.
- (33) Rickwood, D.; Hames, B. D. *Gel Electrophoresis of Nucleic Acids: A Practical Approach*. In *Gel Electrophoresis of Nucleic Acids: A Practical Approach*, 2nd ed.; IRL: Oxford, 1990; p 125.
- (34) Cohen, A. S.; Najarian, D. R.; Paulus, A.; Guttman, A.; Smith, J. A.; Karger, B. L. *Proc. Natl. Acad. Sci. U.S.A.* **1988**, *85*, 9660–3.
- (35) Demorest, D.; Dubrow, R. J. *Chromatogr.* **1991**, *559*, 43–56.
- (36) Guttman, A.; Cohen, A. S.; Heiger, D. N.; Karger, B. L. *Anal. Chem.* **1990**, *62*, 137–41.
- (37) Paulus, A.; Gassmann, E.; Field, M. J. *Electrophoresis* **1990**, *11*, 702–8.
- (38) Paulus, A.; Ohms, J. I. *J. Chromatogr.* **1990**, *507*, 113–123.
- (39) Oefner, P. J.; Bonn, G. K.; Huber, C. G.; Nathakarnkitkool, S. J. *Chromatogr.* **1992**, *625*, 331–40.
- (40) Warren, W. J.; Vella, G. *Methods in molecular biology (Clifton, N.J.)* **1994**, *26*, 233–64.
- (41) Warren, W. J.; Vella, G. *Mol. Biotechnol.* **1995**, *4*, 179–99.
- (42) Ueda, M.; Kiba, Y.; Abe, H.; Arai, A.; Nakanishi, H.; Baba, Y. *Electrophoresis* **2000**, *21*, 176–80.
- (43) Batsberg, W.; Ndoni, S.; Trandum, C.; Hvidt, S. *Macromolecules* **2004**, *37*, 2965–2971.
- (44) Oh, K. T.; Bronich, T. K.; Kabanov, A. V. *J. Controlled Release* **2004**, *94*, 411–422.
- (45) Zhang, J.; Wang, Y. M.; Liang, D. H.; Ying, Q. C.; Chu, B. *Macromolecules* **2005**, *38*, 1936–1943.
- (46) Provencher, S. W. *Comput. Phys. Commun.* **1982**, *27*, 229–242.
- (47) Provencher, S. W. *Makromol. Chem., Macromol. Chem. Phys.* **1979**, *180*, 201–209.
- (48) Liu, T. B.; Xie, Y.; Chu, B. *Langmuir* **2000**, *16*, 9015–9022.
- (49) Liu, T.; Liang, D.; Song, L.; Nace, V. M.; Chu, B. *Electrophoresis* **2001**, *22*, 449–458.
- (50) Zhang, J.; He, W. D.; Liang, D. H.; Fang, D. F.; Chu, B.; Gassmann, M. J. *Chromatogr. A* **2006**, *1117*, 219–227.
- (51) Zhou, Z.; Chu, B.; Nace, V. M. *Langmuir* **1996**, *12*, 5016–5021.
- (52) Ogston, A. G. *Trans. Faraday Soc.* **1958**, *54*, 1754.
- (53) Grossman, P. D.; Soane, D. S. *Biopolymers* **1991**, *31*, 1221–1228.
- (54) De Gennes, P. G. *Scaling Concepts in Polymer Physics*; Cornell University Press: Ithaca, NY, 1979; p 324.

MA070554N